LUMINESCENCE DATING OF LOESS DEPOSITS FROM THE REMAGEN-SCHWALBENBERG SITE, WESTERN GERMANY

NICOLE KLASEN[1], PETER FISCHER[2], FRANK LEHMKUHL[3], ALEXANDRA HILGERS[1]

[1]*Institute of Geography, University of Cologne, Albertus-Magnus-Platz, D-50923 Cologne, Germany*
[2]*Institute for Geography, Johannes-Gutenberg-Universität, Johann-Joachim-Becher-Weg 21, D-55099 Mainz, Germany*
[3]*Department of Geography, RWTH Aachen University, Templergraben 55, D-52056 Aachen, Germany*

Abstract: This study describes the luminescence characteristics of quartz of Upper Pleistocene loess of the Middle Rhine area. The loess/palaeosol sequence of the Schwalbenberg near Remagen comprises a multitude of interstadial soils and soil sediments that have been dedicated to the Marine Isotope Stage 3 (MIS 3). These weak calcaric cambisols and their derivates are underlain by loess and soil sediments of MIS 4 to MIS 5 and covered by loess sediments and intercalated gelic gleysols of MIS 2. We applied luminescence dating of quartz and feldspar of drill core samples and observed an age discrepancy within both data sets. The quartz ages were clearly younger than the feldspar ages, because of thermally unstable signal components of the quartz luminescence signal. Therefore, we regarded the quartz samples of the lower parts of the drill core as unsuitable for luminescence dating. This underestimation did not affect the quartz samples of the upper part of the drill core which was indicated by age control that was provided by the Eltville tephra layer. Geochemical analysis based on X-ray fluorescence showed that the sediments in the upper part and the lower part of the drill core have different geogenic finger prints most likely due to changing source areas of dust and sediment allocation. We assumed that these different facies types were the reason for the luminescence behavior of the quartz samples.

Keywords: luminescence dating, loess, last glacial cycle, Middle Rhine, Eltville tephra, geochemical analysis.

1. INTRODUCTION

Luminescence dating techniques are frequently used for age determination of loess/palaeosol sequences. First studies concentrated on thermoluminescence dating (TL) of polymineral fine grains (4–11 μm) (cf. Wintle, 1981; Zöller and Wagner, 1990). Later, polymineral fine grains were optically stimulated by infrared light (infrared stimulated luminescence dating, IRSL) (cf. Li and Wintle, 1992; Musson and Wintle, 1994; Frechen and Dodonov,

1998; Frechen 1999). IRSL stimulation of polymineral fine grains or feldspar may suffer from D_e underestimation due to anomalous fading (cf. Wintle, 1973). Hence, an increasing number of studies worked on optically stimulated luminescence (OSL) dating of quartz using either fine grain (e.g. Roberts, 2008; Timar *et al.*, 2010), middle grain of 38–63 μm (e.g. Lai, 2006; Roberts, 2006; Stevens *et al.*, 2007) or even fine sand of 63–90 μm (Buylaert *et al.*, 2007), depending on the grain size available. Generally, grain sizes < 63 μm are dominating loess deposits. The limiting factor of dating loess sequences using quartz is the lower saturation dose of the OSL signal. Studies on Romanian loess have shown that dating quartz using different grain sizes of the same sample

Corresponding author: N. Klasen
e-mail: nicole.klasen@uni-koeln.de

resulted in different ages (Timar-Gabor *et al.*, 2011). Kreutzer *et al.* (2012) assumed different transport processes and luminescence characteristics to be causal for differing OSL ages.

The Schwalbenberg loess/palaeosol sequence is considered as a key section for understanding environmental changes during the last glacial cycle within the western European loess belt. The existing chronology of the study site is based on TL, IRSL and post infrared IRSL (pIR IR) dating (Frechen and Schirmer, 2011; Zöller *et al.*, 1991) and the correlation with GISP 2 (Grootes and Stuiver, 1997; in Schirmer, 2012) and the GISP Summit ice core (Dansgaard *et al.*, 1993, in Schirmer *et al.*, 2012). We collected samples from cores that were drilled approximately 200 m northwest of the formerly investigated outcrop (Frechen and Schirmer, 2011) towards the watershed position between the catchments of the Ahr River in the south and a dry valley (Großes Tal), north of the Schwalbenberg (**Fig. 1**).

The purpose of this study was to establish a quartz chronology of the Remagen-Schwalbenberg site to elude feldspar dating which is generally prone to anomalous fading (cf. Wintle, 1973; Thomsen *et al.*, 2008). The Eltville tephra which was dated at several sites to roughly ~20 ka with TL, OSL and IRSL dating (Hatté *et al.*, 1999; Antoine *et al.*, 2001; Zöller *et al.*, 2004; Bibus *et al.*, 2007; Tissoux *et al.*, 2010) and a fluvial terrace at the bottom of the profile which was dedicated to MIS 6 based on its elevation (tr$_9$ after Bibus, 1980, 1983; Lower Middle Terrace after Boenigk and Frechen, 2006) served as chronological markers (**Fig. 2**).

2. SAMPLING SITE

The Schwalbenberg site is located south of the city of Remagen in the Middle Rhine Valley on the left bank of the Rhine River (**Fig. 1**). The transition from the Weichselian Lower Terrace to the loess covered Middle Terrace (dedicated to the penultimate glaciation, eg. Bibus, 1980; Schirmer, 1990; Boenigk and Frechen, 2006) north of the Ahr River is marked by a distinctive slope. The loess covered Middle Terrace is dissected by several dry valleys. The outcrop of former investigations (e.g. Bibus, 1980; Schirmer, 1990, 2000, 2012; Frechen and Schirmer, 2011; Schirmer *et al.*, 2012) is located at the southeastern edge of the Schwalbenberg which forms a plateau-like relief form. From the outcrop to the watershed the elevation increases from approximately 93 m above sea level (a.s.l.) to 107 m a.s.l. The drill core REM 1 (**Fig. 1**) is located at 98.8 m a.s.l. While the formerly investigated outcrop (Frechen and Schirmer, 2011; Schirmer, 2012) comprised a loess sequence of 13 m, the drill core exposed a loess sequence above the fluvial gravels of 20.8 m thickness. Thus, the top of the fluvial terrace is at about 78 m a.s.l. which fits well with the elevation of 79 m a.s.l. given by Boenigk and Frechen (2006) for the top of the Lower Middle Terrace (LMT) at the same site. The chronostratigraphical position of the LMT is based on its
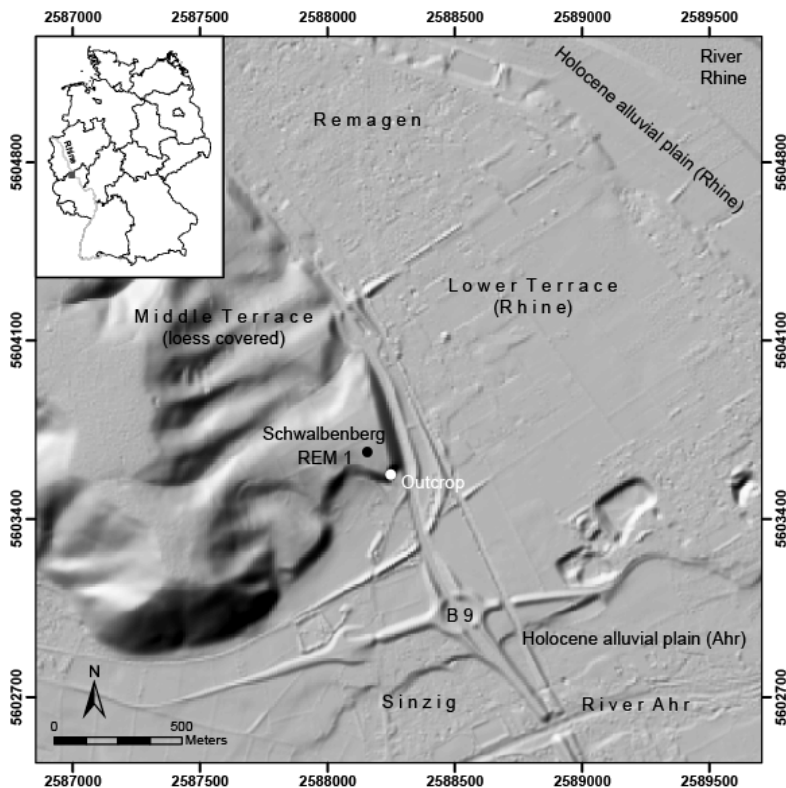

Fig. 1. *Location of drill core REM 1 at the Schwalbenberg site south of Remagen. The transition from the Lower terraces of the Rhine River to the loess covered Middle terraces west of the Schwalbenberg is marked by a distinct cliff. The loess cover of the Middle terraces is dissected by numerous dry valleys. (Data source: DGM 5, Geobasisdaten, Land Surveying and Registry Office of Rhineland-Palatinate (Vermessungs- und Katasterverwaltung Rheinland-Pfalz), 2012).*
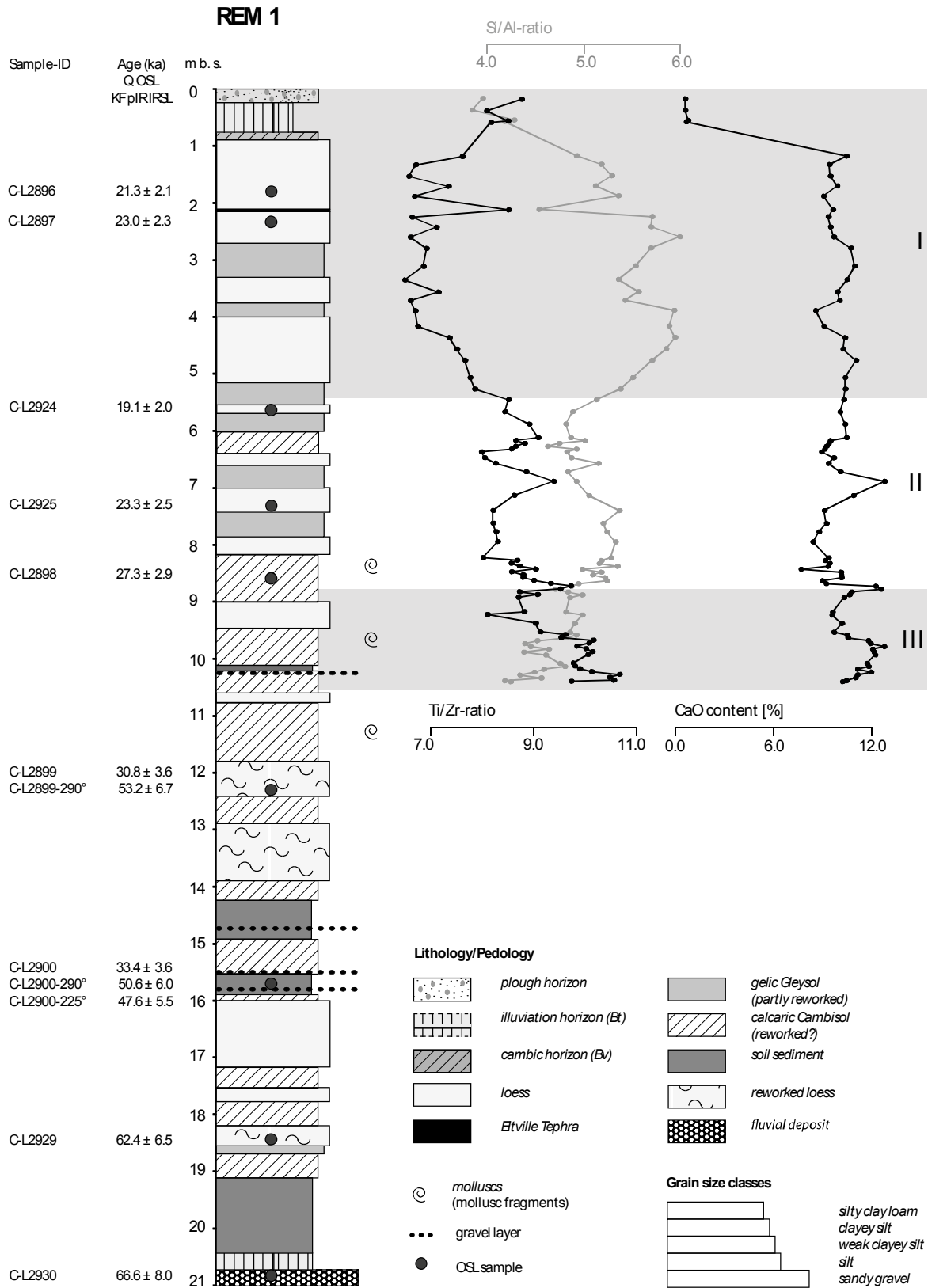
REM 1

Fig. 2. *Litho- and pedological composition, luminescence samples, calculated ages and selected geochemical parameters of drill core REM 1 from the Schwalbenberg site. Light grey and white bars indicate geochemical units (see text for explanation). Grain size classes refer to the sedimentolog-ical-pedological core description. Note that the calcaric cambisols are assumed to be reworked especially in the lower part of the section.*

morphological position in context to stratigraphically older and younger terraces and on constraints provided by the stratigraphical investigation of the loess-palaeosol-sequence on top. At first, Bibus (1980) observed a multitude of intercalated brownish soils in the loess sequence on top of the Lower Middle Terrace (t_{r9} after Bibus, 1980, 1983). It is important to note that Bibus (1980) already considered reworking processes to be responsible for this unique number of brownish soils. In contrast, Schirmer (2012, 2013) and Schirmer *et al.* (2012) assumed that the eight interstadial soils which are part of the Ahrgau-Subformation have been autochthonous soils which reflect climate fluctuations during MIS 3.

3. METHODS

Luminescence dating

Nine samples were collected from a drill core (diameter of 6 cm) under subdued red light conditions. Chemical treatment with HCl (10%), H_2O_2 (10%) and sodium oxalate was applied to remove carbonates, organic material and clay. The middle grain quartz fraction (40–63 µm) was extracted with fluorosilicic acid (35%, two weeks) plus a final HCl wash (10%, one hour). All measurements were carried out on an automated Risø TL/OSL DA 20 reader equipped with a ^{90}Sr beta source delivering ~0.097 Gy/s. Blue light emitting diodes (470 nm) and a Hoya U 340 filter (7.5 mm) transmitting wavelengths of 330 ± 40 nm were used for optical stimulation and signal detection of the quartz multi-grain aliquots (1 mm). The single-aliquot regenerative-dose approach (SAR) was used for all measurements (cf. Murray and Wintle, 2003). Preheat temperatures between 180 and 280°C for 10 s, a cut heat temperature of 20°C below the preheat temperature and OSL stimulation for 50 s at 125°C were employed for the preheat plateau test (C-L2896, C-L2900) and the dose recovery experiment (given doses of 68 Gy (C-L2896) and 82 Gy (C-L2900) 1 mm, 5 aliquots for each temperature). The net OSL signal of the quartz samples was obtained using the initial 1.0 s of the luminescence signal minus a mean background of the last 5 s for all measurements. To further investigate the quartz OSL characteristics, $D_e(t)$ plots (Bailey, 2003; Bailey *et al.*, 2003) were executed for all samples by changing the signal integration interval while the background interval was kept constant to 5 s. Additionally, pulse annealing experiments (180–400°C) using linear modulated OSL (LM OSL, Bulur *et al.*, 2000) were made on samples C-L2896 and C-L2900. The natural OSL signal was reset by OSL stimulation (170°C for 6000 s) in the Risø reader followed by laboratory irradiation (72 Gy). Subsequently the aliquot was preheated and the regenerated LMOSL signal was recorded for 1000 s (a second linear modulated stimulation served for background subtraction) followed by OSL stimulation (170°C for 6000 s) to completely reset the luminescence signal. A test dose (36 Gy) was applied and the subsequent test dose LMOSL was

recorded after preheating to 240°C. This measurement cycle was repeated for preheat temperatures between 180–400°C during the regenerative cycle (cf. Singarayer, 2002). Linear modulated (LM) and continuous wave (CW) OSL curve fitting was carried out using the *fit_LMCurve()* and *fit_CWCurve()* functions of the R package *Luminescence* (version 0.3.2) (Kreutzer *et al.*, 2012).

Coarse grain potassium feldspar (63–100 µm and 100–150 µm) was separated with heavy liquid density separation ($\rho = 2.58$ gcm^{-3}). Post infrared IRSL (pIRIR) stimulation (880 nm) was applied for two samples and an interference filter (410 nm) was used for signal detection of the multi-grain feldspar aliquots (1 mm). The elevated temperature pIRIR signal was expected to be non- or less-fading (Thomsen *et al.*, 2008). The signal was measured at 290°C (pIRIR$_{290}$, Thiel *et al.*, 2011) because anomalous fading was expected to be least for this temperature. For comparison, the pIRR signal was also measured at 225°C (pIRIR$_{225}$, Buylaert *et al.*, 2009) for sample C-L2900 only, because not enough sample material was left for sample C-L2899. To carry out a dose recovery test, feldspar samples were illuminated for 24 h in a Hönle SOL2 solar simulator before they were irradiated (given dose 138 Gy) and subsequently measured with the standard protocols of Thiel *et al.* (2011) and Buylaert *et al.* (2009). Additionally, a bleaching experiment was carried out on the feldspar samples (24 h illumination in a Hönle SOL2 solar simulator) to quantify the amount of the residual signal. The net pIRIR signal was obtained using the initial 4 s and background subtraction of the last 20 s. Data analysis was executed with the Risø Luminescence Analyst software (version 3.24) for quartz and feldspar samples. The SAR criteria of recycling ratio limit (10%), test dose error (10%) and signal >3 sigma above background were applied to reject aliquots from the distribution. Mean equivalent doses were calculated with the central age model (CAM) of Galbraith *et al.* (1999) whereat at least 25 aliquots that passed the SAR acceptance criteria were used. The environmental dose rate was measured using high resolution gamma ray spectrometry. The dose rate was calculated using conversion factors of Guerin *et al.* (2011), alpha and beta attenuation factors of Bell (1980) and Brennan (2003) and the measured water content. For K-feldspars, an internal potassium content of $12.5 \pm 0.5\%$ (Huntley and Baril, 1997) was assumed. The cosmic dose rate was calculated after Prescott and Hutton (1994).

Geochemical analysis

The samples were sieved to the fraction < 63 µm and dried at 105°C for 12 hours to determine the element concentrations of the fine grain fractions. An 8 g quantity of the sieved material was mixed with 2 g of Fluxana Cereox, homogenised and pressed to a pellet with a pressure of 20 tons for 120 s. All samples were measured twice by polarisation energy dispersive X-ray fluores-

cence (EDPXRF) using a Spectro Xepos device. Measurements were conducted in a pre-calibrated mode (38 KeV, 10 W). Mean values were calculated from the two measurements (according to SPECTRO, 2007).

Element concentrations of aluminium (Al), calcium (Ca), titanium (Ti), zirconium (Zr) and silicon (Si) were used for further interpretation. Ti and Al are hardly soluble and thus relatively immobile, which leads to an enrichment during mineral weathering (e.g. Kabata-Pendias, 2011; Zech *et al.*, 2008). In addition both elements are adsorbed to an increasing degree to clay minerals during proceeding silicate weathering. Additionally to weathering, the Ti/Zr ratio indicated changes in the sediment source area as these elements appear in hardly soluble minerals (Muhs *et al.*, 2003). Hence, such ratios based on immobile elements were expected to yield information about changes in the original dust composition (cf. Zech *et al.*, 2008).

4. RESULTS

Litho- and pedological profile composition

The drill core REM 1 (**Fig. 2**) comprised a loess/palaeosol sequence of 20.8 m on top of fluvial gravels, which were correlated to the Lower Middle terrace of the penultimate glaciation (Bibus, 1980; Schirmer, 2012; sample C-L2930). The slightly reworked Bt-horizon on top of these fluvial sediments exposed intensive hydromorphic staining followed by reddish, clay rich soil sediments with intercalated thin loess layers. A first stack of four cambic horizons that was separated by loess sediments and an intensively bleached gelic gleysol was developed above the reworked soil sediments. Sample C-L2929 originates from loess deposits showing lamination due to reworking processes. On top of this part of the sequence strong erosion and sediment relocation was indicated between 15.8 m and 14.2 m by reddish, clay rich soil sediments and the presence of three distinctive gravel layers. In between the upper two gravel layers remains of a cambic horizon occured. Sample C-L2900 was taken between the lower two gravel layers out of the soil sediments. From 14.2 m up to 6 m another six layers were identified displaying characteristics of calcaric cambisol formation. Up to 11.8 m the intercalated loess deposits showed clear lamination which indicated reworking processes as well as a distinctive gravel layer at 10.3 m. Sample C-L2899 originates from the upper reworked loess deposit. Towards the brownish horizon between 6.2 m and 6 m depth, two gelic gleysols separated the loess deposits. This sediment appeared to be less effected by post-sedimentary relocation. Sample C-L2898 was taken directly out of a cambic horizon and sample C-L2925 derived from a loess layer at 7.4 m. Sample C-L2924 postdated the sequence of brownish soils or soil sediments. Four gelic gleysols that have been correlated to the Erbenheim soils 1–4 (Schönhals *et al.*, 1964) and the Eltville-Tephra in a depth of 2.15 m divided the upper

6 m of the loess sequence. The uppermost meter is characterised by a truncated luvisol of the late glacial to Holocene soil formation. The eluviation-horizon (Al) and parts of the illuviation-horizon (Bt) were eroded. Based on field evidence and macroscopic core description twelve layers were distinguished that showed pedogenic superimposition of loess sediments in terms of cambisol formation and secondary carbonate precipitation. In addition, especially for the lower part of the sequence (from 10.3 m downwards) distinct reworking processes were observed.

Luminescence dating

Nine samples were collected from the drill core from loess deposits and the underlying fluvial sediments. The measurements exposed bright feldspar pIRIR signals of the 1 mm aliquots (**Fig. 3a**).The laboratory dose exhibited to feldspar samples C-L2899 and C-L2900 was recovered for the pIRIR$_{290}$ signal within 10% of unity (ratio
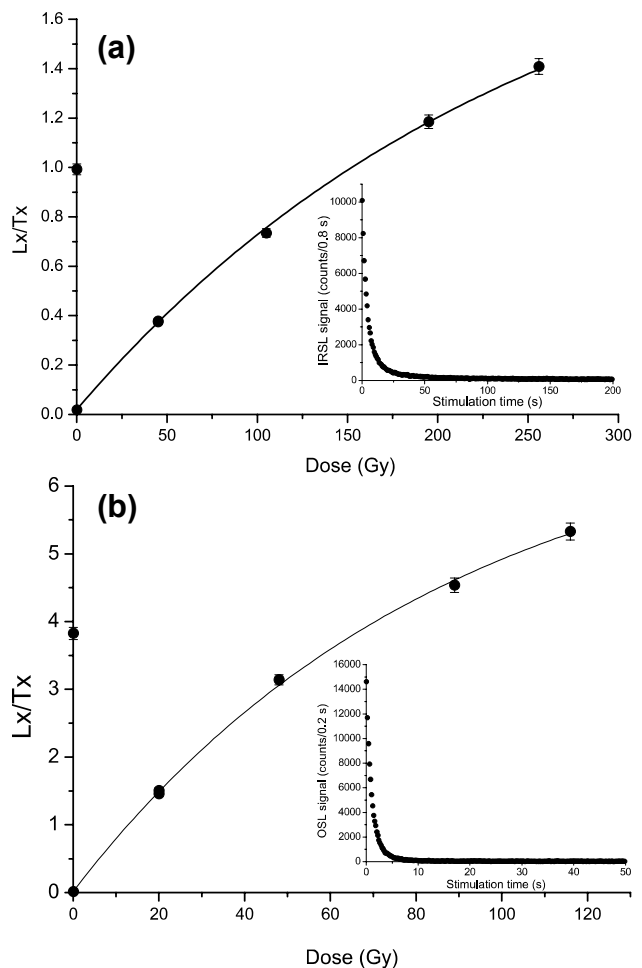

Fig. 3. *Signal intensities (inset) and fitted dose response curves (single saturation exponential) of natural aliquots (1 mm) of feldspar sample C-L2900 (a) and quartz sample C-L2897 (b). The recycling ratios were 1.01 ± 0.03 (C-L2900) and 1.02 ± 0.05 (C-L2897).*

1.05 ± 0.04 and 1.04 ± 0.05). The pIRIR$_{290}$ ages were calculated to 53 ± 7 ka (C-L2899) and 51 ± 6 ka (C-L2900).

First measurements of the multi-grain (1 mm) quartz samples exposed relatively weak luminescence signals with a rapid signal decay (**Fig. 3b**). A preheat temperature of 260°C was selected for all measurements according to the results of the preheat plateau test and the dose recovery test (**Fig. 4**). The two uppermost samples (C-L2896 and C-L2897) that surround the Eltville tephra showed quartz ages between 21 ka and 23 ka and the subjacent samples resulted in ages between 19 ka and 68 ka that were in stratigraphic order (**Table 1**).

We observed that quartz and feldspar ages of the samples C-L2899 and C-L2900 differed significantly from each other. D$_e$(t) plots of the quartz samples identified fallen plateaus for all quartz samples from 5.7 m depth downwards in the section (**Fig. 5**). In contrast, the D$_e$(t) plots of the two uppermost samples displayed a flat plateau (**Fig. 5**). The natural LM OSL signal was fitted to four components for samples C-L2896, C-L2897 and C-L2900 (**Fig. 6a–c**). The average photoionisation cross-sections (σ) of all analysed aliquots (n = 15) were of the same order of magnitude as the values published by Jain *et al.* (2003) and Singarayer and Bailey (2003) and were consecutively named to $\sigma_{fast} = 2.01 \pm 0.05 \times 10^{-17}$ cm^2, $\sigma_{medium} = 8.16 \pm 0.46 \times 10^{-18}$ cm^2, $\sigma_{slow1} = 3.55 \pm 0.16 \times 10^{-19}$ cm^2 and $\sigma_{slow2} = 3.49 \pm 0.12 \times 10^{-20}$ cm^2.

Pulse annealing experiments carried out on sample C-L2900 indicated a stable fast component and thermally unstable medium and slow components of the regenerated quartz OSL signal from 180°C onward (**Fig. 7a**). In contrast, regenerated signals of sample C-L2896 showed a stable fast component and thermal stability of the medi-

um component up to 220°C (**Fig. 7b**). Deconvolution of the continuous wave (CW) OSL signal of sample C-L2900 demonstrated that the natural OSL signal was dominated by the fast component, but the regenerative signals were dominated by the medium component and the ratio of the fast and the medium component altered in the course of the SAR sequence (**Fig. 8**).
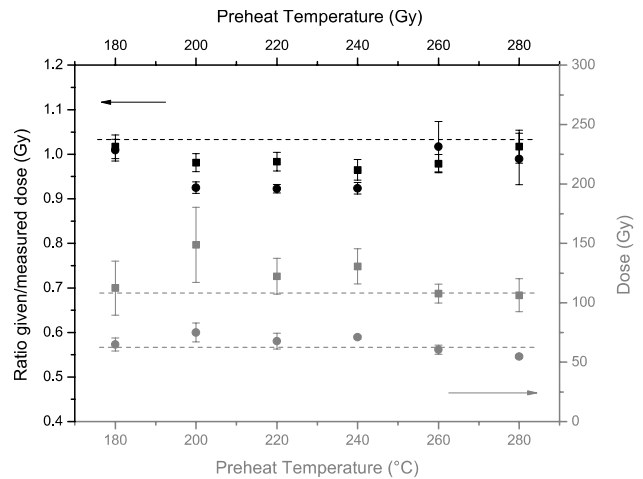

Fig. 4. *Preheat plateau test and dose recovery test of quartz samples C-L2900 (squares) and C-L2896 (circles) (1 mm aliquot, 5 aliquots each temperature). The laboratory given doses of 68 Gy and 82 Gy were reproduced for all temperatures within 10% of unity. A preheat temperature of 260°C (ratio measured to given dose of 1.02 ± 0.06 (C-L2896) and 0.98 ± 0.02 (C-L2900) was selected for all further measurements of the quartz samples.*

Table 1. *Dose rate data, dose distribution characteristics, D$_e$ values (1 mm aliquot) and OSL ages. SD = sample depth; m b. s. = meters below surface; Q = quartz; KF = potassium feldspar; H$_2$O% = measured water content (water mass over dry sediment mass); a/m = accepted/measured; U = Uranium; Th = Thorium; K = Potassium; environmental dose rate is calculated using cosmic dose calculation after Prescott and Hutton (1994), conversion factors of Guerin et al. (2011), beta attenuation factors of Brennan (2003); internal K-content of 12.5 ± 0.5% (Huntley and Baril, 1997) and the measured water content; OD = overdispersion value; RSD = relative standard deviation; D$_e$ = equivalent dose; * = feldspar age based on the pIRIR$_{225}$ signal measured. The quartz ages from below 2.3 m depth are regarded as unreliable due to thermally unstable components of the OSL signal.*

| Sample ID	SD (m b.s.)	mineral	H$_2$O (%)	n a/m aliquots	Radionuclide concentration			Dose rate (Gy/ka)	OD (%)	RSD (%)	D$_e$ Q (Gy)	Age Q (ka)
					U (ppm)	Th (ppm)	K (%)					
C-L2896	1.8	Q	9	47/61	2.80 ± 0.14	9.97 ± 0.63	1.33 ± 0.05	2.72 ± 0.32	13 ± 0.6	17	57.9 ± 3.1	21.3 ± 2.1
C-L2897	2.3	Q	9	48/61	2.85 ± 0.15	9.78 ± 0.57	1.36 ± 0.05	2.75 ± 0.32	10 ± 0.4	12	63.1 ± 3.3	23.0 ± 2.3
C-L2924	5.7	Q	11	32/42	2.55 ± 0.13	9.11 ± 0.53	1.39 ± 0.05	2.63 ± 0.30	20 ± 1.1	22	50.3 ± 3.1	19.1 ± 2.0
C-L2925	7.4	Q	11	41/60	2.80 ± 0.14	9.61 ± 0.55	1.37 ± 0.05	2.69 ± 0.28	28 ± 1.7	32	60.8 ± 4.1	22.6 ± 2.4
C-L2898	8.6	Q	15	35/69	2.64 ± 0.14	9.02 ± 0.53	1.37 ± 0.05	2.57 ± 0.32	26 ± 1.6	27	70.4 ± 4.7	27.3 ± 2.9
C-L2899	12.3	Q	14	37/61	2.49 ± 0.13	8.42 ± 0.49	1.22 ± 0.05	2.29 ± 0.27	38 ± 2.7	41	70.9 ± 5.7	30.9 ± 3.6
C-L2899	12.3	KF	14	25/26	2.49 ± 0.13	8.42 ± 0.49	1.22 ± 0.05	2.51 ± 0.30	25 ± 1.7	29	140.8 ± 9.9	56.0 ± 3.9
C-L2900	15.7	Q	18	36/60	2.63 ± 0.14	9.97 ± 0.58	1.52 ± 0.06	2.73 ± 0.29	30 ± 2.1	31	91.3 ± 6.6	33.4 ± 3.6
C-L2900	15.7	KF	18	28/28	2.63 ± 0.14	9.97 ± 0.58	1.52 ± 0.06	2.79 ± 0.31	20 ± 1.2	27	153.9 ± 9.7	55.2 ± 3.5
C-L2900	15.7	KF	18	23/28	2.63 ± 0.14	9.97 ± 0.58	1.52 ± 0.06	2.79 ± 0.31	13 ± 0.8	14	144.8 ± 8.3	51.9 ± 3.0*
C-L2929	18.5	Q	20	38/53	2.65 ± 0.13	9.13 ± 0.52	1.39 ± 0.05	2.56 ± 0.27	22 ± 1.4	26	159.6 ± 10.1	62.4 ± 6.5
C-L2930	20.8	Q	17	33/54	2.87 ± 0.14	10.92 ± 0.62	1.84 ± 0.07	2.96 ± 0.35	41 ± 3.4	42	201.3 ± 18.0	67.9 ± 8.0
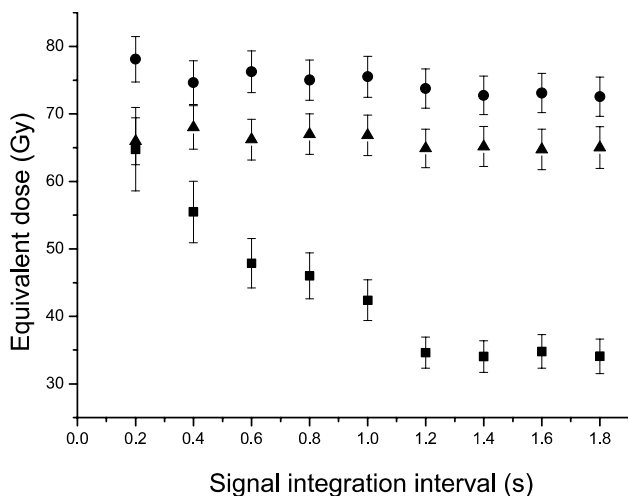
Fig. 5. *$D_e(t)$ plot of one aliquot of quartz samples C-L2896 (circles), C-L2897 (triangles) and C-L2900 (squares). The channel width is 0.2 s and the signal integration interval was changed while the background interval was kept constant to 5 s. The error bars represent the individual D_e errors for the integrated signal. A fallen D_e with increasing stimulation time was observed for sample C-L2900 only. This indicates thermally unstable components of the luminescence signal.*

Geochemical analysis

High resolution geochemical data were available for the upper 10.4 m of the sequence.

The element concentrations and calculated ratios (**Fig. 2**) indicated a subdivision of this part of the loess/palaeosol sequence into three geochemical units which were characterised by significant shifts in curve progression.

Apart from the truncated luvisol on top of the sequence that is decalcified, the CaO values were characterised by a weak variation of ~ 10 ± 2%. A distinct peak occured towards the base of the gelic gleysol in a depth of 7 m and towards the base of the second cambic horizon in 8.8 m. Slightly higher values were also observed towards the base of the analytical sequence most likely because of secondary carbonate precipitation on top of the clay rich soil sediment and the underlying gravel layer in a depth of 10.2 m. In view to the Ti/Zr- and Si/Al ratios reverse curve progression was visible for the whole analytical sequence (**Fig. 2**). The upper part of unit I reflected the soil formation within the truncated luvisol and showed distinct peaks for the Eltville tephra layer. From 4.4 m down to 5.4 m the values of Ti/Zr increased while Si/Al values decreased. Unit II ranged from 5.4 m to 8.8 m. The above mentioned maximum peak of the CaO-content in 7 m depth was accompanied by a maximum in the Ti/Zr-ratio.
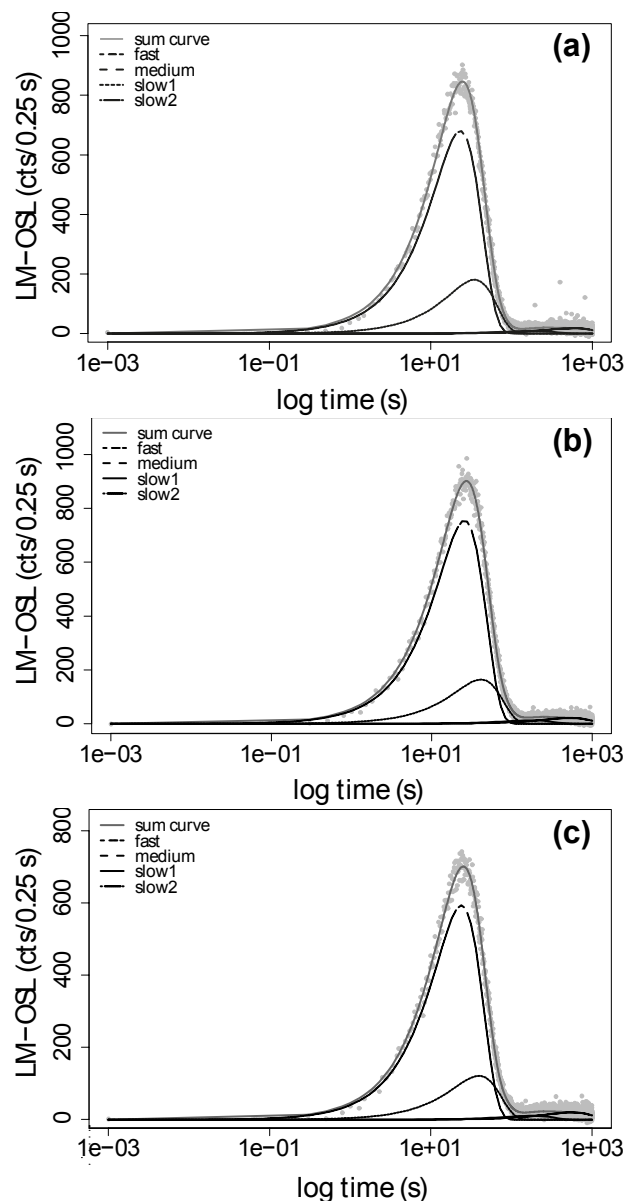

Fig. 6. *Linear modulated OSL signal of samples C-L2896 (a), C-L2897 (b) and C-L2900 (c). The natural signal (n = 6) was fitted to four components using the R software package "Luminescence" (version 0.3.2) (Kreutzer et al., 2012).*

Towards the base of unit II and within unit III significant fluctuations in both element ratios and in the CaO-content were observed. The cambic horizons were characterised by distinct maxima of the Ti/Zr ratio and minima of the Si/Al ratio and the intercalated loess layers showed the inverse signal.
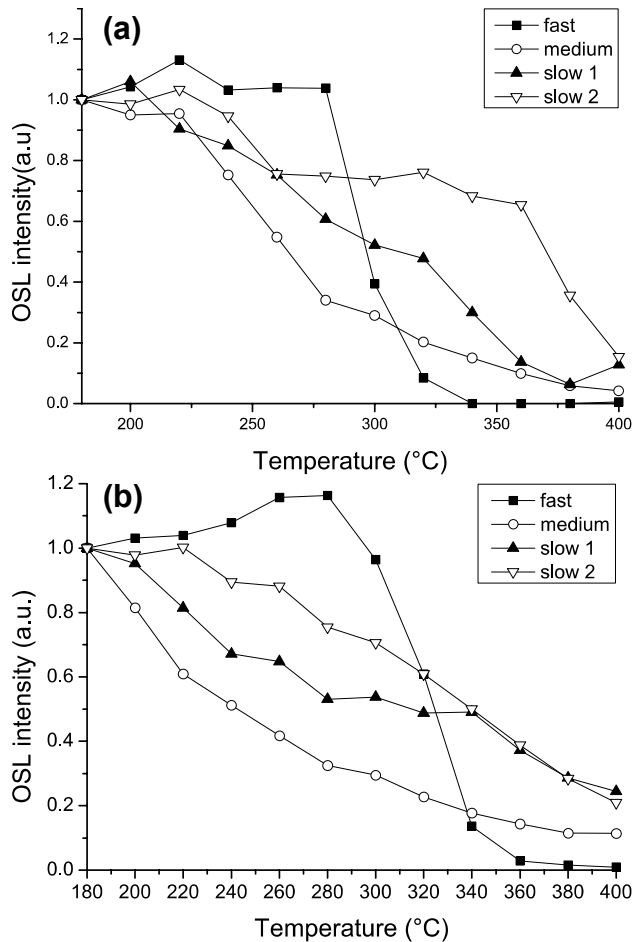
Fig. 8. *The continuous wave signal of sample C-L2900 was deconvolved into its individual components for every OSL signal (natural and regenerative doses). The ratio of the fast component and the medium component is plotted for the individual SAR cycles. The ratio changes during the course of the SAR cycle. The fast component dominates only the natural signal and the 4th regenerative signal which proved that these samples are not suitable for OSL dating using SAR techniques.*

Fig. 7. *Thermal stability of samples C-L2896 (a) and C-L2900 (b). The fast component is thermally stable up to 280°C for C-L2900 and up to 300°C for C-L2896. The medium component shows thermal instability from 180°C on (C-L2900) and above 220°C for sample C-L2896. This is different to the results of the $D_e(t)$ plot for sample C-L2896 which did not show any decrease with increasing stimulation time.*

5. DISCUSSION

The luminescence ages obtained from the 20.8 m drill core using quartz (40–63 μm) point to a sedimentation during the last glacial cycle from MIS 4 to MIS 2. The upper two samples surround the Eltville tephra which was dated to ~20 ka with TL, OSL and IRSL dating at several sites in Germany and Belgium (Pouclet and Juvigne, 2009). This is in accordance with the quartz ages of 21–23 ka (C-L2896, C-L2897) for the samples above and below the tephra.

In contrast, two quartz ages in the lower parts of the drill core varied from the two feldspar ages of the same samples (C-L2899, C-L2900) by about 20 ka (**Table 1**). Moreover, the lowermost sample that derived from the fluvial terrace at the bottom of the section and that was dedicated to MIS 6 (e.g. Bibus, 1980; Boenigk and Frechen, 2006; Frechen and Schirmer, 2011; Schirmer,
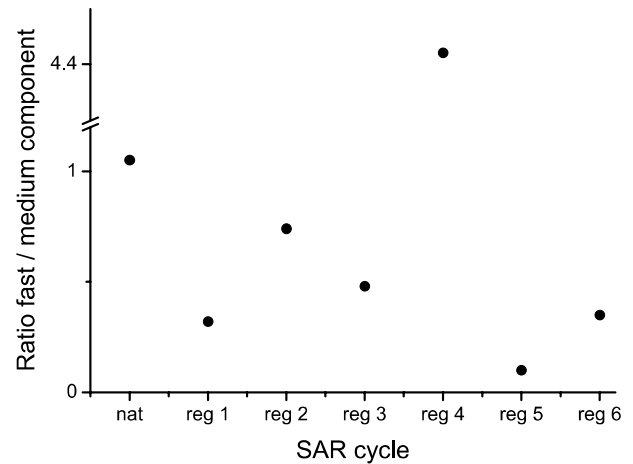
2012) yielded a quartz age of 67 ± 8 ka (C-L2930). Compared with the existing chronostratigraphy, the quartz ages from the lower parts of the drill core were clearly younger than expected. We assessed the quartz ages to be underestimated because of thermally unstable luminescence signal components (**Fig. 5**, **7b**). Similar differences between quartz and feldspar ages because of unstable signal components of the quartz signal were reported by Shen and Mauz (2009), Steffen *et al.* (2009) or Tsukamoto *et al.* (2003).

Continuous wave curve fitting analysis exposed that the ratio of the fast component to the medium component changed from the natural to the regenerative luminescence signals (**Fig. 8**, cf. Steffen *et al.*, 2009). The thermal instability of the signal components was crucial and therefore, we considered the OSL ages unreliable. Geochemical analysis indicated that different sediment facies that reflect changes in the source area were accumulated. We assumed that this was the reason for the different luminescence behaviour of the samples from the upper and the lower part of the drill core. The data set showed a distinct shift in a depth of 5.4 m (boundary from unit I to unit II, **Fig. 2**) which was characterised by decreasing values of the Si/Al ratio and increasing values of the Ti/Zr ratio accompanied by constant values of the CaO content. Intensive weathering for this part of the sequence was excluded based on core description and constant CaO values. Although comparison to other possible source areas of sediment allocation has not been conducted so far, the shift in geochemical composition certainly reflects differences in the geogenic background of the lo-

ess/palaeosol sequence. Based on litho- and pedological evidence this shift most likely marks the transition from MIS 3 to MIS 2. Possibly, the sequence from 5.4 m downwards carried a dominating local signature in view to the sediment source.

A quick deposition of the sediments between 12 and 16 m depth was indicted by the pIRIR ages. In combination with the observed evidence for strong reworking processes, small scale sediment (and soil) relocation cannot be excluded to be causal for the unique thickness of the sequence and the number of soil and soil sediments.

Likewise, Frechen and Schirmer (2011) discussed near distance sediment transport at least for the lower part of the investigated sequence. The luminescence ages of the lowermost 3.2 m of the sequence yielded IRSL and TL ages between about 55 and 50 ka at the base and fading corrected IRSL and pIRIR ages of about 54 and 55 ka at the top, respectively (Frechen and Schirmer, 2011) which points to sedimentation during MIS 3 and MIS 2. In addition the ages of the Ahrgau-Subformation showed no significant increase with depth which also indicated a rapid sediment accumulation (Frechen and Schirmer, 2011). On the contrary, the core described in this study yielded greater sediment thickness and a more detailed stratigraphy for the deposits dedicated to MIS 2 (including the Eltville Tephra layer). Moreover, the sequence which has been dedicated to MIS 3 showed four more layers owing to characteristics of cambisol formation and at least the feldspar ages (C-L2899, C-L2900) fit well with the existing chronology of Frechen and Schirmer (2011).

All existing age estimates from the Schwalbenberg site point to a rapid accumulation of loess, reworked loess and soil sediments during MIS 3 and MIS 2. Based on litho- and pedological aspects (higher organic carbon content and increased weathering indices of the palaeosols), Schirmer (2012) and Schirmer *et al.* (2012) interpreted the loess sequence as a mirror picture of climate signals similar to Greenland ice core stratigraphies. A delayed response of depositional, erosional and soil formation processes to climate changes can only be assumed because of the unreliable quartz ages that were presented in this study. We think it still has to be discussed, if the Schwalbenberg loess-palaeosol sequence really is the mirror picture of MIS 3.

6. CONCLUSION

The aim of this study was to establish a quartz chronology of a loess/palaeosol sequence obtained in a drill core at the Schwalbenberg site near Remagen. We showed that the quartz ages were unreliable because of unfavourable luminescence characteristics of seven out of nine quartz samples. Two feldspar ages from the sequence were in good agreement with the existing feldspar chronology of Frechen and Schirmer (2011) but no new

chronological findings were achieved in this study. The uppermost quartz samples that surrounded the Eltville Tephra layer showed appropriate luminescence characteristics. This indicated that different sediment facies account for the specific luminescence behavior. These different facies were also detected by geochemical analysis. The great advantage of the present sampling strategy was that drilling allowed to conduct transects towards the watershed position. This provided material for further luminescence dating studies to further investigate the genesis and landscape evolution of the Remagen-Schwalbenberg site. All data produced so far showed the necessity of establishing accumulation models including sediment sources as well as the determination of spatial and temporal changes in the geomorphological system and associated driving factors.

REFERENCES

Antoine P, Rousseau DD, Zöller L, Lang A, Munaut AV, Hatté C and Fontugne M, 2001. High-resolution record of the last Interglacial-glacial cycle in the Nussloch loess-palaeosol sequences, Upper Rhine Area, Germany. *Quaternary International* 76–77: 211–229, DOI 10.1016/S1040-6182(00)00104-X.

Bailey RM, 2003. Paper I: The use of measurement-time dependent single-aliquot equivalent-dose estimates from quartz in the identification of incomplete signal resetting. *Radiation Measurements* 37(6): 673–683, DOI 10.1016/S1350-4487(03)00078-7.

Bailey RM, Singarayer JS, Ward S and Stokes S, 2003. Identification of partial resetting using De as a function of illumination time. *Radiation Measurements* 37(6): 511–518, DOI 10.1016/S1350-4487(03)00063-5.

Bell WT, 1980. Alpha dose attenuation in quartz grains for thermoluminescence dating. *Ancient TL 12*: 4–8.

Bibus E, 1980. Zur Relief-, Boden- und Sedimententwicklung am unteren Mittelrhein. (Relief, soil and sediment genesis of the Lower Middle Rhine). *Frankfurter Geowissenschaftliche Arbeiten* Serie D, 1. Frankfurt: 296pp (in German).

Bibus E, 1983. Distribution and Dimension of Young Tectonics in the Neuwied Basin and the Lower Middle Rhine. *Plateau Uplift*: 55–61.

Bibus E, Frechen M, Kösel M and Rähle W, 2007. Das jungpleistozäne Lössprofil von Nussloch (SW Wand) im Aufschluss der Heidelberger Zement AG. (The Late Pleistocene loess profile Nussloch (SW wall). *Eiszeitalter und Gegenwart* 56: 227–255 (in German).

Boenigk W and Frechen M, 2006. The Pliocene and Quaternary fluvial archives of the Rhine system. *Quaternary Science Reviews* 25(5–6): 550–574, DOI 10.1016/j.quascirev.2005.01.018.

Brennan BJ, 2003. Beta doses to spherical grains. *Radiation Measurements* 37(4–5): 299–303, DOI 10.1016/S1350-4487(03)00011-8.

Bulur E, Bøtter-Jensen L and Murray AS, 2000. Optical stimulated luminescence from quartz measured using the linear modulation technique. *Radiation Measurements* 32(5–6): 407–411, DOI 10.1016/S1350-4487(00)00115-3.

Buylaert JP, Murray AS, Thomsen KJ and Jain M, 2009. Testing the potential of an elevated temperature IRSL signal from K-feldspar. *Radiation Measurements* 44(5–6): 560–565, DOI 10.1016/j.radmeas.2009.02.007.

Buylaert JP, Vandenberghe D, Murray AS, Huot S, De Corte F and Van den Haute P, 2007. Luminescence dating of old (>70ka) Chinese loess: a comparison of single aliquot OSL and IRSL techniques. *Quaternary Geochronology* 2(1–4): 9–14, DOI 10.1016/j.quageo.2006.05.028.

Dansgaard W, Johnsen SJ, Clausen HB, Dahl-Jensen D, Gundestrup NS, Hammer CU, Hvidberg CS, Steffensen JP, Sveinbjørnsdottir AE, Jouzel J and Bond G, 1993. Evidence for general instability of past climate from a 250-kyr ice-core record. *Nature* 364: 218–220, DOI 10.1038/364218a0.

Frechen M, 1999. Upper Pleistocene loess stratigraphy in Southern Germany. *Quaternary Science Reviews* 18(2): 243–269, DOI 10.1016/S0277-3791(98)00058-4.

Frechen M and Dodonov AE, 1998. Loess chronology of the Middle and Upper Pleistocene in Tadjikistan. *Geologische Rundschau* 87: 2–20.

Frechen M and Schirmer W, 2011. Luminescence chronology of the Schwalbenberg II loess in the Middle Rhine valley. *Quaternary Science Journal* 60(1): 78–89, DOI 10.3285/eg.60.1.05.

Galbraith RF, Roberts RG, Laslett GM, Yoshida H and Olley JM, 1999. Optical dating of single and multi-grains of Quartz from Jinmium rock shelter, northern Australia: Part I, experimental design and statistical models. *Archaeometry* 41(2): 339–364, DOI 10.1111/j.1475-4754.1999.tb00987.x.

Grootes PM and Stuiver M, 1997. Oxygen 18/16 variability in Greenland snow and ice with 10^{-3} to 10^5-year time resolution. *Journal of Geophysical Research* 102(C12): 26455–26470, DOI 10.1029/97JC00880.

Guerin G, Mercier, N and Adamiec, G, 2011. Dose-rate conversion factors: update. *Ancient TL* 29(1): 5–8.

Hatté C, Antoine P, Fontugne M, Rousseau DD, Tisnerat-Laborde N and Zöller L, 1999. New chronology and organic matter δ13C paleoclimatic significance of Nussloch loess sequence (Rhine Valley, Germany). *Quaternary International* 62(1): 85–91, DOI 10.1016/S1040-6182(99)00026-9.

Huntley DJ and Baril MR, 1997. The K content of the K-feldspars being measured in optical dating or in thermoluminescence dating. *Ancient TL* 15(1): 11–13.

Jain M, Murray AS and Bøtter-Jensen L, 2003. Characterisation of blue-light stimulated luminescence components in different quartz samples: implications for dose measurement. *Radiation Measurements* 37(4–5): 441–449, DOI 10.1016/S1350-4487(03)00052-0.

Kabata-Pendias A, 2011. *Trace elements in soils and plants*. CRC Press, Boca Raton: 548pp.

Kreutzer S, Fuchs M, Meszner S and Faust D, 2012. OSL chronology of a loess-palaeosol sequence in Saxony/Germany using quartz of different grain sizes. *Quaternary Geochronology* 10: 102–109, DOI 10.1016/j.quageo.2012.01.004.

Lai ZP, 2006. Testing the use of an OSL standardised growth curve (SGC) for De determination on quartz from the Chinese Loess Plateau. *Radiation Measurements* 41(1): 9–16, DOI 10.1016/j.radmeas.2005.06.031.

Li SH and Wintle AG, 1992. A global view of the stability of Luminescence signals from loess. *Quaternary Science Reviews* 11(1–2): 133–137, DOI 10.1016/0277-3791(92)90054-C.

Muhs DR, Ager TA, Bettis EA, McGeehin J, Been JM, Beget JE, Pavich MJ, Stafford TW and Stevens DSP, 2003. Stratigraphy and palaeoclimatic significance of Late Quaternary loess-palaeosol sequences of the Last Interglacial-Glacial cycle in central Alaska. *Quaternary Science Reviews* 22(18–19): 1947–1986, DOI 10.1016/S0277-3791(03)00167-7.

Murray AS and Wintle AG, 2003. The single aliquot regenerated dose protocol: potential for improvements in reliability. *Radiation Measurements* 37(4–5): 377–381, DOI 10.1016/S1350-4487(03)00053-2.

Musson FM and Wintle AG, 1994. Luminescence dating of the loess profile at Dolní Vestonice, Czech Republic. *Quaternary Science Reviews* 13(5–7): 411–416, DOI 10.1016/0277-3791(94)90051-5.

Pouclet A and Juvigne E, 2009. The Eltville tephra, a late Pleistocene widespread tephra layer in Germany, Belgium and the Netherlands; symptomatic compositions of the minerals. *Geologica Belgica* 12: 93–103.

Prescott JR and Hutton JT, 1994. Cosmic ray contributions to dose rates for luminescence and ESR dating: large depth and long-term time variations. *Radiation Measurements* 23(2–3): 497–500, DOI 10.1016/1350-4487(94)90086-8.

Roberts HM, 2006. Optical dating of coarse-silt sized quartz from loess: evaluation of equivalent dose determinations and SAR procedural checks. *Radiation Measurements* 41(7–8): 923–929, DOI 10.1016/j.radmeas.2006.05.021.

Roberts HM, 2008. The development and application of luminescence dating to loess deposits: a perspective on the past, present and future. *Boreas* 37(4): 483–507, DOI 10.1111/j.1502-3885.2008.00057.x.

Schirmer W, 1990. Schwalbenberg südlich Remagen. In: Schirmer, W. (Ed.), Rheingeschichte zwischen Mosel und Maas. (History of the Rhine River between Moselle River and Meuse River) *Deuqua-Führer* 1, 94–98 (in German).

Schirmer W, 2000. Eine Klimakurve des Oberpleistozäns aus dem rheinischen Löss. (Climate record of the Upper Pleistocence of the loess from the Rhine River). *Eiszeitalter und Gegenwart* 50: 25–49.

Schirmer W, 2012. Rhine loess at Schwalbenberg II - MIS 4 and 3. *Eiszeitalter und Gegenwart (Quaternary Science Journal)* 61(1): 32–47, DOI 10.3285/eg.61.1.03.

Schirmer W, Ikinger A and Nehring F, 2012. Die terrestrischen Böden im Profil Schwalbenberg/Mittelrhein. (Terrestrial soils of the Schwalbenberg profile/Middle Rhine). *Mainzer Geowissenschaftliche Mitteilungen* 40: 53–78 (in German).

Schirmer W, 2013. Ahrgau-Subformation. *In LithoLex [http://www.bgr.bund.de/litholex; online-database]*. Hannover: BGR. Last updated 13.03.2013. [cited 16.12.2014]. Record No. 1000027.

Schönhals E, Rohdenburg H and Semmel A, 1964. Ergebnisse neuerer Untersuchungen zur Würmlößgliederung in Hessen (New investigations on the chronology of the Wuermian loess in Hesse). *Eiszeitalter und Gegenwart* 15: 199–206 (in German).

Shen Z and Mauz B, 2009. De determination of quartz samples showing fallen De(t) plots. *Radiation Measurements* 44(5–6): 566–570, DOI 10.1016/j.radmeas.2009.06.003.

Singarayer JS, 2002. Linearly modulated optically stimulated luminescence of sedimentary quartz: physical machanisms and implications for dating. *PhD thesis, University of Oxford, Oxford*: 345pp.

Singarayer JS and Bailey RM, 2003. Further investigation s of the quartz optically stimulated luminescence components using linear modulation. *Radiation Measurements* 37(4–5): 451–458, DOI 10.1016/S1350-4487(03)00062-3.

SPECTRO (eds.), 2007. Analysis of Trace Elements in Geological Materials, Soils and Sludges Prepared as Pressed Pellets. *SPECTRO XRF Report*, XRF-39.

Steffen D, Preusser F and Schlunegger F, 2009. OSL quartz age underestimation due to unstable signal components. *Quaternary Geochronology* 4(5): 353–362, DOI 10.1016/j.quageo.2009.05.015.

Stevens T, Armitage SJ, Lu H and Thomas DSG, 2007. Examining the potential of high sampling resolution OSL dating of Chinese loess. *Quaternary Geochronology* 2(1–4): 15–22, DOI 10.1016/j.quageo.2006.03.004.

Thiel C, Buylaert JP, Murray AS and Tsukamoto S, 2011. On the applicability of post-IR IRSL dating to Japanese loess. *Geochronometria* 38(4): 369–378, DOI 10.2478/s13386-011-0043-4.

Thomsen KJ, Murray AS, Jain M and Bøtter-Jensen L, 2008. Laboratory fading rates of various luminescence signals from feldspar-rich sediment extracts. *Radiation Measurements* 43(9–10): 1474–1486, DOI 10.1016/j.radmeas.2008.06.002.

Timar-Gabor A, Vandenberghe DAG, Vasiliniuc S, Panaoitu CE, Panaiotu CG, Dimofte D and Cosma C, 2011. Optical dating of

Romanian loess: A comparison between silt-sized and sand-sized quartz. *Quaternary International* 240: 62–70, DOI 10.1016/j.quaint.2010.10.007.

Timar A, Vandenberghe D, Panaiotu EC, Panaiotu CG, Necula C, Cosma C and Van den Haute P, 2010. Optical dating of Romanian loess using fine-grained quartz. *Quaternary Geochronology* 5: 143–148, DOI 10.1016/j.quageo.2009.03.003.

Tissoux H, Valladas H, Voinchet P, Reyss JL, Mercier N, Falguères C, Bahain JJ, Zöller L and Antoine P, 2010. OSL and ESR studies of Aeolian quartz from the Upper Pleistocene loess sequence of Nussloch (Germany). *Quaternary Geochronology* 5: 131–136, DOI 10.1016/j.quageo.2009.03.009.

Tsukamoto S, Rink WJ and Watanuki T, 2003. OSL of tephric loess and volcanic quartz in Japan and an alternative procedure for estimation *D*e from a fast OSL component. *Radiation Measurements* 37(4–5): 459–465, DOI 10.1016/S1350-4487(03)00054-4.

Wintle AG, 1973. Anomalous fading of thermoluminescence in mineral samples. *Nature* 245: 143–144, DOI 10.1038/245143a0.

Wintle AG, 1981. Thermoluminescence dating of Late Devensian loesses in southern England. *Nature* 289: 479–480, DOI 10.1038/289479a0.

Zech M, Zech R, Zech W, Glaser B, Brodowski S and Amelung W, 2008. Characterisation and palaeoclimate of a loess-like permafrost palaeosol sequence in NE Siberia. *Geoderma* 143(3–4): 281–295, DOI 10.1016/j.geoderma.2007.11.012.

Zöller L and Wagner GA, 1990. Thermoluminescence datingf loess - recent developments. *Quaternary International* 7–8: 119–128, DOI 10.1016/1040-6182(90)90046-7.

Zöller L, Conard NJ and Hahn J, 1991. Thermoluminescence dating of Middle Palaeolithic open air sites in the Middle Rhine Valley/Germany. *Naturwissenschaften* 78(9): 408–410.

Zöller L, Rousseau DD, Jäger KD and Kukla G, 2004. Last interglacial, Lower and Middle Weichselian - a comparative study from the Upper Rhine and Thuringian loess area. *Zeitschrift für Geomorphologie* 48(1): 1–24.